

Contents lists available at ScienceDirect

Acta Biomaterialia

journal homepage: www.elsevier.com/locate/actbio



Full length article

An *in vitro* hyaluronic acid hydrogel based platform to model dormancy in brain metastatic breast cancer cells



Akshay A. Narkhede ^{a,1}, James H. Crenshaw ^{a,1}, David K. Crossman ^b, Lalita A. Shevde ^c, Shreyas S. Rao ^{a,*}

- ^a Department of Chemical and Biological Engineering, The University of Alabama, Tuscaloosa, AL 35487-0203, USA
- ^b Department of Genetics, University of Alabama at Birmingham, Birmingham, AL, USA
- ^c Department of Pathology, O'Neal Comprehensive Cancer Center, University of Alabama at Birmingham, Birmingham, AL, USA

ARTICLE INFO

Article history: Received 20 November 2019 Revised 19 February 2020 Accepted 25 February 2020 Available online 29 February 2020

Keywords: Cancer dormancy Breast cancer brain metastasis In vitro model Hyaluronic acid (HA) hydrogel

ABSTRACT

Breast cancer cells (BCCs) can remain dormant at the metastatic site, which when revoked leads to formation of metastasis several years after the treatment of primary tumor. Particularly, awakening of dormant BCCs in the brain results in breast cancer brain metastasis (BCBrM) which marks the most advanced stage of the disease with a median survival period of ~4-16 months. However, our understanding of dormancy associated with BCBrM remains obscure, in part, due to the lack of relevant in vitro platforms to model dormancy associated with BCBrM. To address this need, we developed an in vitro hyaluronic acid (HA) hydrogel platform to model dormancy in brain metastatic BCCs via exploiting the bio-physical cues provided by HA hydrogels while bracketing the normal brain and metastatic brain malignancy relevant stiffness range. In this system, we observed that MDA-MB-231Br and BT474Br3 brain metastatic BCCs exhibited a dormant phenotype when cultured on soft (0.4 kPa) HA hydrogel compared to stiff (4.5 kPa) HA hydrogel as characterized by significantly lower EdU and Ki67 positivity. Further, we demonstrated the nuclear localization of p21 and p27 (markers associated with dormancy) in dormant MDA-MB-231Br cells contrary to their cytoplasmic localization in the proliferative population. We also demonstrated that the stiffness-based dormancy in MDA-MB-231Br cells was reversible and was, in part, mediated by focal adhesion kinases and the initial cell seeding density. Finally, RNA sequencing confirmed the dormant phenotype in MDA-MB-231Br cells. This platform could further our understanding of dormancy in BCBrM and could be adapted for anti-metastatic drug screening.

Statement of Significance

Our understanding of dormancy associated with BCBrM remains obscure, in part, due to the lack of relevant *in vitro* platforms to model dormancy associated with BCBrM. Herein, we present a HA hydrogel-based platform to model dormancy in brain metastatic BCCs while recapitulating key aspects of brain microenvironment. We demonstrated that the biophysical cues provided the HA hydrogel mediates dormancy in brain metastatic BCCs by assessing both proliferation and cell cycle arrest markers. We also established the role of focal adhesion kinases and initial cell seeding density in the stiffness-mediated dormancy in brain metastatic BCCs. Further, RNA-seq. confirmed the dormant phenotype in brain metastatic BCCs. This platform could be utilized to further our understanding of microenvironmental regulation of dormancy in BCBrM.

© 2020 Acta Materialia Inc. Published by Elsevier Ltd. All rights reserved.

1. Introduction

Breast cancer can progress to form metastasis at secondary organ sites such as bones, lungs, liver and the brain several years after surgical resection of the primary tumor [1]. Approximately, 67% of deaths in case of breast cancer occur past the 5-year survival period, largely owing to disease relapse at the metastatic site [2–4].

^{*} Corresponding author.

E-mail address: srao3@eng.ua.edu (S.S. Rao).

¹ These author contributed equally to the work.

This latency period between the treatment of primary tumor and relapse has been attributed to dormancy [2,3,5,6]. Disseminated breast cancer cells may remain in a dormant state at the metastatic site for extended periods of time, which when revoked leads to metastasis [2,3,5,6]. Specifically, reawakening of dormant breast cancer cells in the brain leads to brain metastasis, which marks the most advanced stage of the disease with a median survival period of ~4–16 months [7,8]. Even with substantial progress in developing therapeutic regimens, these metastatic breast cancer cells remain refractory to current therapeutics [8]. Therefore, an improved understanding of the biology of these dormant metastatic breast cancer cells is urgently needed. However, this has been hindered, in part, due to the lack of relevant *in vitro* experimental models to study dormancy in brain metastatic breast cancer cells [1].

It is well appreciated that the tumor microenvironment plays a significant role in cancer dormancy [2,5]. Therefore, it is important for an in vitro dormancy model to capture the bidirectional crosstalk between the microenvironment and cancer cells. Specifically, the extracellular matrix (ECM) is one of the key components of tumor microenvironment which provides cancer cells with bio-physical/-chemical cues, hence, mediating the dormant phenotype [2,5,9,10]. To understand the mechanisms of microenvironmental regulation of dormancy in breast cancer, experimental in vitro models have been developed. For example, 3D Cultrex® basement membrane extract was employed as an in vitro model to examine dormancy in mouse mammary cancer cells [11-14]. Similarly, models using poly(ε -caprolactone) electrospun scaffolds [15], laminin-rich ECM [16], Transglutaminase-crosslinked collagen gels (Col-Tgel) [17], Fibrin hydrogels [18,19], poly (ethylene glycol) (PEG) hydrogels [10] and amikacin hydrate-based hydrogels (Amikagel) [20] have been devised to study dormancy in primary cancer cells. In the context of breast cancer metastasis, models of dormancy include biomaterial-based models (Gelfoam) [21,22] and bioreactorbased models for bone metastasis [23]; co-culture-based models [24,25] and a combination of co-culture and polyethylene glycol diacrylate hydrogel biomaterial-based model [26] for liver metastasis.

Mouse models, including experimental metastasis mouse models, have also been used for dormancy studies [27,28]; however, controlled investigations using such models is challenging as they provide very limited control of the organ environment [2]. Further, high costs, animal-animal variations, as well as the difficulties involved in imaging dormant cancer cells in tissues makes their use relatively challenging [2]. Whereas some scientific advances have been made in studying dormancy in primary and metastatic breast cancer cells *in vitro*, to the best of our knowledge, experimental *in vitro* models to study dormancy in brain metastatic breast cancer cells in a controlled setting have not been reported.

To address this unmet need, herein, we report a hyaluronic acid (HA) hydrogel platform, as an in vitro model to study dormancy in brain metastatic breast cancer cells. We chose HA hydrogel platform as HA is a major component of the brain ECM and is highly expressed in brain metastatic tissue [7,29,30]. In addition, HA is known to interact with metastatic breast cancer cells via CD44 receptors [7,29]. Herein, we engineered mechanically soft and stiff HA hydrogels while bracketing the normal brain and metastatic brain malignancy relevant stiffness range. We cultured brain metastatic breast cancer cells on top of HA hydrogels to study regulation of the dormant phenotype via exploiting the bio-physical cues provided by soft and stiff HA hydrogels. We also investigated the role of focal adhesion kinases (FAK) and the initial cell seeding density in stiffness-mediated dormancy in brain metastatic breast cancer cells. Finally, we investigated the differential gene expression in cells cultured on soft vs. stiff HA hydrogels through RNA sequencing.

2. Materials and methods

2.1. HA hydrogel preparation

HA hydrogels were prepared as described in our earlier work [7]. Briefly, HA (66-90 kDa; Lifecore Biomedical) (in 1 wt% aqueous solution) was methacrylated by reacting it with ~18-fold molar excess of methacrylic anhydride (Sigma Aldrich) while maintaining pH>8 at 4°C, to yield hyaluronic acid methacrylate (HAMA) with ~85% degree of methacrylation, as determined through proton nuclear magnetic resonance (¹H NMR) [7,31]. To prepare soft and stiff HA hydrogels, a hydrogel precursor solution containing 5 wt% HAMA and crosslinker Dithiothreitol (DTT) (Sigma Aldrich) at a final concentration of 10 mM for soft and 40 mM for stiff HA hydrogels was prepared in serum-free Dulbecco's Modified Eagle's Medium (DMEM) (Sigma Aldrich). 75 µL of hydrogel precursor solution was added to each well of a 96-well plate and incubated overnight to form hydrogels. This resulted in hydrogels with stiffnesses of ~0.4 kPa (soft) and ~4.5 kPa (stiff), respectively, as determined through compression testing performed on RSA-G2 solid analyzer instrument (TA Instruments) [7]. To provide cell adhesion sites, surfaces of both soft and stiff HA hydrogels were consistently functionalized with the integrin binding peptide (RGD) (Anaspec) through Michael type addition reaction as described previously [7]. Briefly, 25 µL of 1 mg/mL RGD solution in serum-free DMEM was added to each well containing soft or stiff HA hydrogels and incubated for 3 hr at room temperature prior to cell seeding.

2.2. Cell culture

td-Tomato (red fluorescent protein; RFP)-expressing MDA-MB-231Br, a brain metastasizing variant of triple negative breast cancer cell line MDA-MB-231, was generously provided by Dr. Lonnie Shea (University of Michigan). MDA-MB-231Br cells were routinely cultured in DMEM supplemented with 10% (v/v) fetal bovine serum (FBS) (VWR Life Science) and 1% (v/v) penicillin-streptomycin at 37 °C and 5% CO₂. BT474Br3, a brain metastasizing variant of human epidermal growth factor receptor 2 (HER2) positive breast cancer cell line BT474 [32], was generously provided by Dr. Dihua Yu (University of Texas MD Anderson Cancer Center). BT474Br3 cells were routinely cultured in DMEM/F12 (1:1) (Gibco; Life Technologies) supplemented with 10% (v/v) fetal bovine serum (FBS) and 1% (v/v) penicillin-streptomycin at 37 °C and 5% CO₂.

2.3. EdU cell proliferation assay

Proliferation of MDA-MB-231Br and BT474Br3 cells on soft and stiff HA hydrogels was evaluated through incorporation of 5-ethynyl-2'-deoxyuridine (EdU) in DNA using Click-iT® EdU microplate assay kit (C10214; Invitrogen). Briefly, 5000 MDA-MB-231Br or BT474Br3 cells were seeded on top of soft and stiff HA hydrogels respectively. At day 2, 10 µM EdU in respective cell culture media was added to each well and the cells were incubated with EdU overnight. At day 3, spent media containing EdU was removed and cells were trypsinized for ~5 min and retrieved from HA hydrogels. The cells were then pelleted and resuspended in 300 µL of 1X PBS (Gibco; Life Technologies). In case of BT474Br3 cells (sphere forming cells), the cell pellet was treated with 200 μL Accutase (Corning) to disintegrate the spheres and yield single cells prior to resuspension in 300 µL of 1X PBS. The cells in 1X PBS were added to a 96-well plate, followed by centrifugation at ~1000 x g for ~15 s for the cells to settle at the bottom following which the spent PBS was removed and the cells were stained for EdU as per the manufacturer's protocol. Briefly, cells were fixed for 5 min at room temperature by adding 50 µL of Click-iT® EdU fixative to each well followed by the addition of 50 µL reaction

cocktail containing Oregon green® 488 azide which binds to the incorporated EdU. The cells were incubated with the reaction cocktail for ~25 min. The plate was then centrifuged at ~1000 x g for ~15 s and the spent reaction cocktail was removed. The cells were washed twice with 1X PBS and counterstained with 4,6-diamidino-2-phenylindole (DAPI) (Invitrogen) nuclear stain. The cells were then imaged using an Olympus IX83 microscope with a spinning disk confocal attachment. Similar exposure time and gain settings were maintained throughout all conditions. Percent EdU positive cells were evaluated through manual counting using multi-point tool in ImageJ software (NIH). A similar approach was used by Marlow et al., wherein the cells were retrieved from the 3D matrix prior to the detection of EdU labeled cells in order to establish dormant vs. proliferative phenotypes [21].

2.4. Immunofluorescence staining

Immunofluorescence staining was performed to investigate the expression of Ki67, marker for cellular proliferation [33] and p21 and p27, markers associated with cell cycle arrest and cancer dormancy [6,34]. For Ki67 staining, 5000 MDA-MB-231Br or BT474Br3 cells were seeded on top of soft and stiff HA hydrogels respectively. At day 3, cells were retrieved from HA hydrogels as described above and added to a 96-well plate. The plate was then centrifuged at ~1000 x g for ~15 s for the cells to settle at the bottom. The cells were then fixed with 4% paraformaldehyde, permeabilized using 0.25% Triton-X in 1X PBS and blocked with 5% BSA in 1X PBS. The cells were then incubated with 1 µg/ml of primary antibody (Anti-Ki67 antibody) (ab15580; abcam) overnight at 4°C followed by incubation with 2 µg/ml of Alexa Fluor 488conjugated goat anti-rabbit secondary antibody (A-11034; Invitrogen) for 45 min. The cells were counterstained with DAPI nuclear stain. The plate was centrifuged at ~1000 x g for ~15 s every time prior to the removal of liquids from wells to avoid the loss of cells. The cells were then imaged using an Olympus IX83 microscope with a spinning disk confocal attachment. Similar exposure time and gain settings were maintained throughout all conditions. Percent Ki67 positive cells were evaluated through manual counting using multi-point tool in ImageJ software (NIH). A similar approach was used by Marlow et al., wherein the cells were retrieved from the 3D matrix prior to Ki67 staining in order to establish dormant vs. proliferative phenotypes [21].

For p21 and p27 staining, 5000 MDA-MB-231Br cells were seeded on top of soft and stiff HA hydrogels respectively. At day 2, the spent media was removed and the cells were gently washed once with 1X PBS. The cells were fixed with 4% paraformaldehyde, permeabilized using 0.25% Triton-X in 1X PBS and blocked with 5% BSA in 1X PBS on the HA hydrogels. The cells were then incubated with primary antibody (1:50 dilution of stock in 1X PBS) for p21 (sc-817; Santa Cruz Biotechnology) or p27 (sc-56338; Santa Cruz Biotechnology) overnight at 4°C on the HA hydrogels, followed by incubation with 2 µg/ml of Alexa Fluor 488-conjugated goat antimouse secondary antibody (A-11001; Invitrogen) for 45 min. The cells were counterstained with DAPI nuclear stain and imaged using an Olympus IX83 microscope with a spinning disk confocal attachment. Percent cells with nuclear localization of p21 and p27 was evaluated through manual counting using multi-point tool in ImageJ software (NIH).

2.5. Focal adhesion kinase (FAK) blocking study

For FAK blocking study, 5000 MDA-MB-231Br cells were seeded on top of stiff HA hydrogels and were treated with varying concentrations of FAK inhibitor 14 (Sigma Aldrich) viz. 0, 1, 2.5, 5, 7.5, 10 and 12.5 μ M respectively throughout the experiment. At day 3, cells were retrieved from stiff HA hydrogels and stained for Ki67

as described above. In a separate setup, MDA-MB-231Br cells on stiff HA hydrogels were treated with FAK inhibitor 14 as described above and were retrieved at day 3 to determine the cellular viability in the presence of varying FAK inhibitor 14 concentrations through trypan blue staining, which was further used to compute percent viable Ki67 negative cells.

2.6. Cell seeding density study

In order to evaluate the impact of cell seeding density on the MDA-MB-231Br phenotype on soft HA hydrogels, initially, 5000, 10,000, 20,000, 35,000 and 50,000 MDA-MB-231Br cells were seeded onto soft HA hydrogels respectively. At day 2, 10 μ M EdU was added to each condition and the cells were incubated with EdU overnight. At day 3, the cells were retrieved from soft HA hydrogels and stained for the incorporated EdU as described above.

2.7. Whole transcriptome RNA sequencing

In order to investigate the differential gene expression in MDA-MB-231Br cells cultured on soft versus stiff HA hydrogels, whole transcriptome RNA sequencing was performed. Briefly, 5000 MDA-MB-231Br cells were seeded onto the soft and stiff HA hydrogels respectively. At day 3, cells were retrieved from soft and stiff HA hydrogels ($n \ge 5$ hydrogels) and lysed to extract total RNA using RNeasy® mini kit (74,104; Qiagen) as per the manufacturer's protocol. mRNA-sequencing was performed on the Illumina NextSeq500 as described by the manufacturer (Illumina Inc., San Diego, CA). Briefly, the quality of the total RNA was assessed using the Agilent 2100 Bioanalyzer. RNA with RNA Integrity Number (RIN) of 7.0 or above was used for sequencing library preparation. The Agilent SureSelect Strand Specific mRNA library kit was used as per the manufacturer's instructions (Agilent, Santa Clara, CA). Library construction began with two rounds of polyA selection using oligo dT containing magnetic beads. The resulting mRNA was randomly fragmented with cations and heat, which was followed by first strand synthesis using random primers with inclusion of Actinomycin D (2.4 ng/µL final concentration). Second strand cDNA production was done with standard techniques and the ends of the resulting cDNA were made blunt, A-tailed and adaptors ligated for indexing to allow for multiplexing during sequencing. The cDNA libraries were quantitated using qPCR in a Roche LightCycler® 480 with the Kapa Biosystems kit for Illumina library quantitation (Kapa Biosystems, Woburn, MA) prior to cluster generation. Cluster generation was performed according to the manufacturer's recommendations for onboard clustering (Illumina). Paired end 75 bp sequencing runs were completed to allow for better alignment of the sequences to the reference genome.

STAR (version 2.7.0b) was used to align the raw RNA-Seq fastq reads to the human reference genome (GRCh38 p7 Release 25) from Gencode [35]. Following alignment, HTSeq-count (version 0.9.1) was used to count the number of reads mapping to each gene [36]. Normalization and differential expression were then applied to the count files using DESeq2 while controlling for batch differences [37]. For generating networks, a data set containing gene identifiers and corresponding expression values was uploaded into Ingenuity Pathway Analysis (IPA). Each identifier was mapped to its corresponding object in Ingenuity's Knowledge Base. A fold change (FC) cut-off of ± 2 and q-value < 0.05 was set to identify molecules whose expression was significantly differentially regulated. These molecules, called Network Eligible molecules, were overlaid onto a global molecular network developed from information contained in Ingenuity's Knowledge Base. Networks of Network Eligible Molecules were then algorithmically generated based on their connectivity. The Functional Analysis identified the biological functions and/or diseases that were most significant to the entire data set. Molecules from the dataset that met the FC cutoff of ± 2 and q-value < 0.05 and were associated with biological functions and/or diseases in Ingenuity's Knowledge Base were considered for the analysis. Right-tailed Fisher's exact test was used to calculate a p-value determining the probability that each biological function and/or disease assigned to that data set is due to chance alone. For heatmaps, the genes that were differentially regulated (FC cut-off of ± 2 and p < 0.05) between soft vs. stiff HA hydrogels were categorized through DAVID gene ontology tool (using the inbuilt functional annotation tool) and IPA. The FPKM values of genes in the chosen enriched gene sets were inputted into an online tool named ClustVis to generate the heat maps [38].

2.8. Statistical analysis

All experiments were repeated at least twice with at least 3 replicates per condition in each experiment. The results are presented as mean \pm standard deviation unless otherwise stated. A t-test was performed (using JMP Pro-software) for comparison of 2 samples belonging to normal datasets. For multiple comparisons in normal datasets, the data was subjected to ANOVA followed by the post-hoc Tukey HSD test (using JMP Pro-software). For non-normal dataset, Wilcoxon each pair test was performed for multiple comparisons (using JMP Pro-software). A p-value less than 0.05 was considered to be statistically significant.

3. Results

3.1. Brain metastatic breast cancer cells exhibit a dormant phenotype when cultured on soft HA hydrogel whereas they proliferate on stiff HA hydrogel

We initially assessed the proliferation of MDA-MB-231Br and BT474Br3 brain metastatic breast cancer cells when cultured on soft (0.4 kPa) and stiff (4.5 kPa) HA hydrogels through incorporation of EdU in the newly synthesized DNA. Incorporation of EdU has been routinely used to assess cell cycle progression (G0/G1 transition) and cancer dormancy [10,21,24,39]. EdU staining at day 3 post cell seeding revealed that the number of EdU positive cells was significantly lower when brain metastatic breast cancer cells were cultured on soft HA hydrogels compared to stiff HA hydrogels (p <0.05) (Fig. 1). In particular, only ~2 ± 6% MDA-MB-231Br cells were EdU positive when cultured on soft HA hydrogels. Similar observation was made in case of BT474Br3 cells wherein only ~5 ± 7% cells were EdU positive when cultured on soft HA hydrogels compared to ~22 ± 11% EdU positive cells on stiff HA hydrogel.

Further, we analyzed Ki67 positivity of MDA-MB-231Br and BT474Br3 cells cultured on soft and stiff HA hydrogels. Ki67 is a proliferation marker which is highly expressed during G2 and mitotic (M) phase of cell cycle [33]. In addition, Ki67 has been used as a marker to study dormancy in several studies [16,21,24]. Ki67 staining at day 3 revealed that the number of Ki67 positive cells was significantly lower when brain metastatic breast cancer cells were cultured on soft HA hydrogels compared to stiff HA hydrogels (p<0.05) (Fig. 2). In particular, only ~6 \pm 5% MDA-MB-231Br cells were Ki67 positive when cultured on soft HA hydrogels. Similar observation was made in case of BT474Br3 cells wherein only ~12 \pm 6% cells were Ki67 positive on soft HA hydrogels compared to ~32 \pm 4% Ki67 positive cells on stiff HA hydrogels. Collectively, these observations indicate a non-proliferative

phenotype in brain metastatic breast cancer cells when cultured on soft HA hydrogels due to arrest in early phase of cell cycle resulting in a dormant phenotype.

We noted differences in the cellular morphologies of MDA-MB-231Br and BT474Br3 cells cultured on soft and stiff HA hydrogels (Suppl. Fig. 1). Specifically, MDA-MB-231Br cells exhibited rounded morphology when cultured on soft HA hydrogel whereas they spread and extended cellular processes when cultured on stiff HA hydrogels and 2D tissue culture polystyrene (TCPS) (Suppl. Fig. 1). Further, cells cultured on stiff HA hydrogel also typically reached confluency by day 3 in stark contrast to the cells cultured on the soft HA hydrogel (Suppl. Fig. 1). BT474Br3 cells formed multicellular aggregates when cultured on both soft and stiff HA hydrogels however, qualitatively, there were more multicellular aggregates on stiff HA hydrogels compared to soft HA hydrogels (Suppl. Fig. 1). Interestingly, BT474Br3 grown on 2D TCPS form multicellular colonies (Suppl. Fig. 1). Early apoptosis assay revealed low apoptotic index in MDA-MB-231Br and BT474Br3 cells on soft and stiff HA hydrogels at day 1 with no significant difference between the groups (p>0.05) (Suppl. Fig. 2, Suppl. Fig. 3). Further, the total cell count in the case of MDA-MB-231Br cells at day 3 (based on automated trypan blue assay) was $\sim 4259 \pm 658$ cells/hydrogel on soft HA hydrogel and ~16,600 \pm 2645 cells/hydrogel on stiff HA hydrogel (initial cell seeding density being ~5000 cells/hydrogel) (Suppl. Fig. 4). This indicates that culturing MDA-MB-231Br cells on soft HA hydrogel halts their proliferation (making them dormant), and further corroborates the observations made through EdU and Ki67 staining. In addition, we observed that the dormant phenotype on soft HA hydrogels was reversible as dormant MDA-MB-231Br cells on soft HA hydrogels exhibited a spread morphology and proliferated when transferred onto stiff HA hydrogels (Suppl. Figs.5 and 6). Further, we observed an enhanced resistance to chemotherapeutic drug Paclitaxel (Taxol) in MDA-MB-231Br cells on soft HA hydrogel compared to stiff HA hydrogel and 2D TCPS as indicated by higher half maximal inhibitory concentration (IC50) however, the difference did not reach statistical significance (p = 0.08) (Suppl. Fig. 7). Taken together, these observations indicate that the brain metastatic breast cancer cells exhibit a dormant (non-proliferative) phenotype on soft HA hydrogels, whereas they exhibit a proliferative phenotype on stiff HA hydrogels, and that the substrate stiffness-driven dormancy is reversible.

3.2. Cyclin-dependent kinase inhibitors p21 and p27 exhibit nuclear localization in MDA-MB-231Br cells cultured on soft HA hydrogels

Cyclin dependent kinase inhibitors p21 and p27 (markers associated with cell cycle arrest) have been previously implicated in cancer dormancy [6,34]. Herein, we examined their expression pattern in MDA-MB-231Br cells cultured on soft and stiff HA hydrogels. We chose MDA-MB-231Br cells for subsequent studies as they exhibited drastic differences in the magnitude of both EdU and Ki67 positivity when cultured on soft vs. stiff HA hydrogels respectively (Fig. 1A,B, Fig. 2A,B). Interestingly, immunofluorescence staining at day 2 revealed nuclear localization of both p21 and p27, in MDA-MB-231Br cells cultured on soft HA hydrogel contrary to their cytoplasmic localization in MDA-MB-231Br cells cultured on stiff HA hydrogel (Fig. 3, Suppl. Fig. 8). In particular, ~89 \pm 8% MDA-MB-231Br cells showed nuclear localization of p21 on soft HA hydrogel compared to only $\sim 9 \pm 8\%$ on stiff HA hydrogel (p < 0.05). Similarly, ~91 \pm 5% MDA-MB-231Br cells showed nuclear localization of p27 on soft HA hydrogel compared to only \sim 3 \pm 4% on stiff HA hydrogel (p < 0.05). Thus, the dormant vs. proliferative phenotype observed in these cells was confirmed by assessing both markers associated with proliferation (i.e., Ki67 and EdU), as well as cell cycle arrest (i.e., p21 and p27).

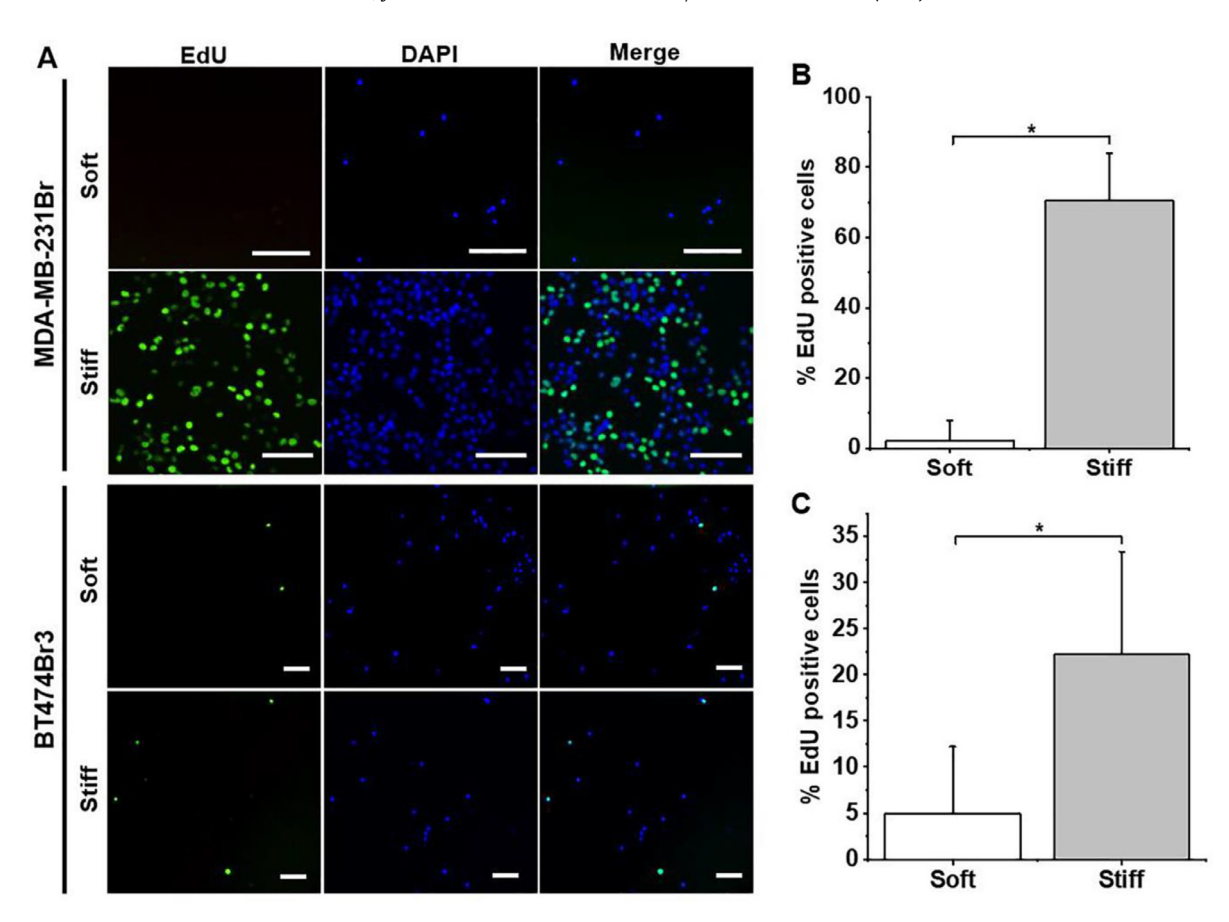


Fig. 1. Brain metastatic breast cancer cells cultured on soft (0.4 kPa) HA hydrogel were largely EdU negative and exhibited a dormant phenotype. A. Representative fluorescence microscopy images of EdU staining at day 3 of MDA-MB-231Br cells (upper panel) and BT474Br3 (lower panel) cultured on soft (0.4 kPa) and stiff (4.5 kPa) HA hydrogel respectively. Green: EdU; Blue: DAPI (nuclei). Scale bar = 100 μ m. B. Quantification of EdU positive MDA-MB-231Br cells cultured on soft and stiff HA hydrogel respectively. N = 6 replicates per condition. * indicates statistical significance (p < 0.05). Error bar represents standard deviation (For interpretation of the references to colour in this figure legend, the reader is referred to the web version of this article.).

3.3. Role of focal adhesion kinases (FAK) in mediating the stiffness-based dormancy in MDA-MB-231Br cells

In our previous work, we demonstrated that focal adhesion kinases (FAK) partly mediate the stiffness-based response of MDA-MB-231Br cells [7]. Particularly, we observed that blocking FAK resulted in a significant reduction in proliferation on stiff HA hydrogels [7]. Further, FAK signaling has been implicated in dormancy, as inhibition of FAK signaling has been shown to induce dormancy in HEp3 human carcinoma cells [40]. Therefore, we investigated the role of FAK in mediating the stiffness-based dormancy in MDA-MB-231Br cells. We hypothesized that blocking FAK in proliferative MDA-MB-231Br cells on stiff HA hydrogels would result in cells exhibiting a more dormant phenotype. To test our hypothesis, we treated MDA-MB-231Br cells with varying concentrations of FAK inhibitor 14 on stiff HA hydrogel and assessed their Ki67 status at day 3. Indeed, we observed that with an increase in the FAK inhibitor concentration, the Ki67 positivity was significantly reduced in MDA-MB-231Br cells on stiff HA hydrogels (Fig. 4A,B) compared to the control group (p < 0.05). Particularly, the Ki67 positivity reduced from ~76 \pm 8% in the control group to ~32 \pm 12% in cells treated with 12.5 µM of FAK inhibitor 14. Recognizing the fact that treatment with FAK inhibitor may impact cellular viability and hence Ki67 positivity; we assessed the cellular viabilities using trypan blue assay and used it to calculate viable Ki67 negative cells (Suppl. Table 1). Interestingly, we observed that with an increase in FAK inhibitor concentration, the number of viable Ki67 negative cells increased significantly compared to the control group

(p < 0.05) (Fig. 4C). Specifically, the percent viable Ki67 negative cells increased from ~7 \pm 5% in control group to ~38 \pm 2% in cells treated with 12.5 μ M of FAK inhibitor 14. The increase in the number of viable Ki67 negative cells indicates an increase in the number of dormant cells on stiff HA hydrogels following FAK inhibition. These results indicated that FAK, in part, mediates the stiffness-based dormancy in MDA-MB-231Br brain metastatic breast cancer cells.

3.4. Initial cell seeding density impacts the dormant phenotype in MDA-MB-231Br cells cultured on soft HA hydrogel

We further evaluated the impact of initial cell seeding density on the dormant phenotype of MDA-MB-231Br cells on soft HA hydrogels. We initially seeded 5000, 10,000, 20,000, 35,000 and 50,000 MDA-MB-231Br cells on soft HA hydrogel and performed EdU staining at day 3. Interestingly, we observed that increasing initial cell seeding density partly revoked the dormant phenotype in MDA-MB-231Br cells on soft HA hydrogel as characterized by an increase in percentage of EdU positive cells (Fig. 5). Specifically, the EdU positivity significantly increased from \sim 2 \pm 4% in 5000 cells per hydrogel condition to ~38 \pm 10% at 50,000 cells per hydrogel (p < 0.05). Increased EdU positivity was also accompanied by some cell spreading on soft HA hydrogels in conditions with higher initial cell seeding densities (Suppl. Fig. 9). No significant difference in the cellular morphologies (in terms of spreading) with varying cell seeding densities were observed in case of BT474Br3 cells (Suppl. Fig. 9).

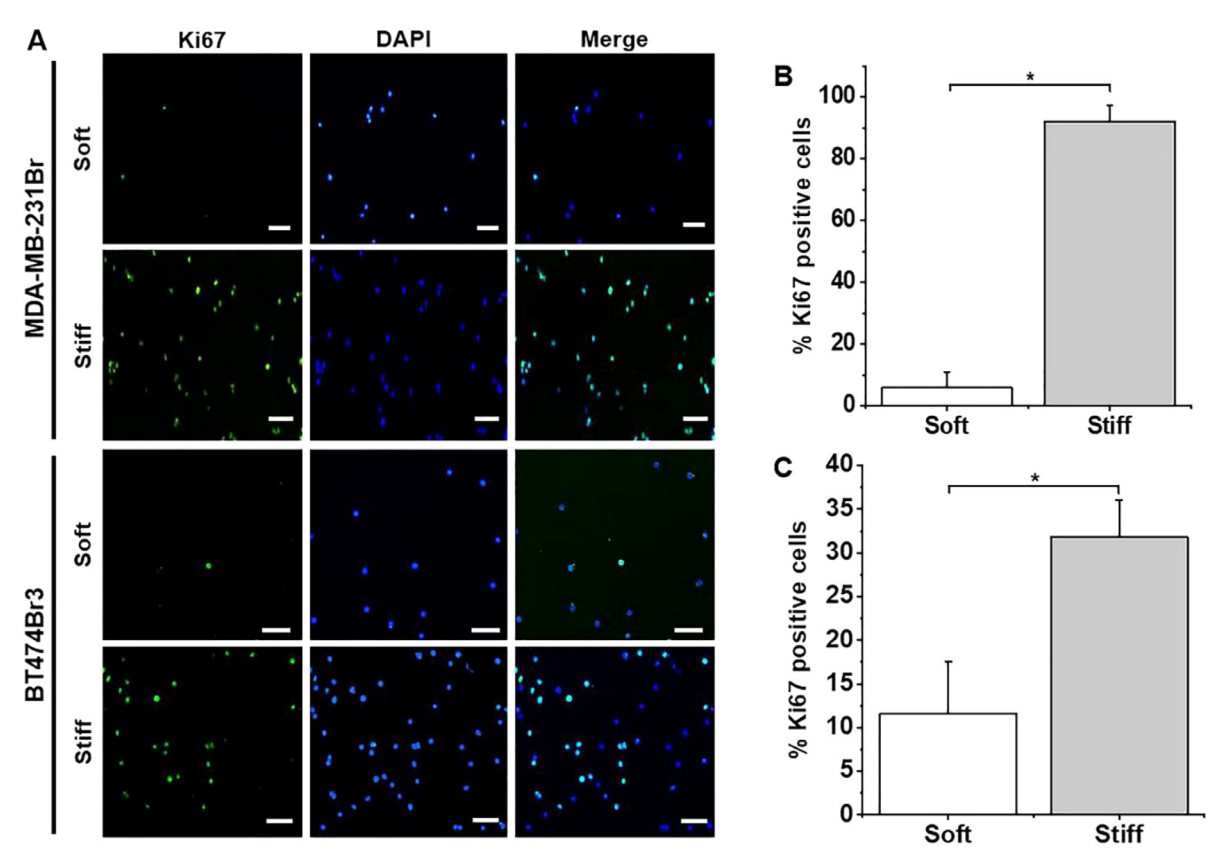


Fig. 2. Brain metastatic breast cancer cells cultured on soft (0.4 kPa) HA hydrogel were largely Ki67 negative and exhibited a dormant phenotype. A. Representative fluorescence microscopy images of Ki67 staining at day 3 of MDA-MB-231Br cells (upper panel) and BT474Br3 (lower panel) cultured on soft (0.4 kPa) and stiff (4.5 kPa) HA hydrogel, respectively. Green: Ki67; Blue: DAPI (nuclei). Scale bar = 100 μm. B. Quantification of Ki67 positive MDA-MB-231Br cells cultured on soft and stiff HA hydrogel respectively. N = 6 replicates per condition. * indicates statistical significance (p<0.05). Error bar represents standard deviation. (For interpretation of the references to colour in this figure legend, the reader is referred to the web version of this article.)

3.5. Differential gene expression in MDA-MB-231Br cells cultured on soft versus stiff HA hydrogels through whole transcriptome RNA sequencing

To associate phenotype with genotype in our model system, we performed whole transcriptome RNA sequencing. Whole transcriptome RNA sequencing revealed that ~1394 genes were differentially regulated between MDA-MB-231Br cells cultured on soft and stiff HA hydrogel respectively (FC cut-off \pm 2, p <0.05) (Supporting file 1). Consistent with our expectations, major gene groups downregulated in MDA-MB-231Br cells cultured on soft HA hydrogel (dormant) compared to MDA-MB-231Br cells on stiff HA hydrogel (proliferative) included genes associated with G1/S transition of mitotic cell cycle and cell division (Fig. 6A, Supporting file 2) (as enriched in DAVID gene ontology tool; p < 0.05). Further, major gene groups upregulated in MDA-MB-231Br cells cultured on soft HA hydrogel (dormant) included genes associated with cell cycle arrest and inflammatory response (Fig. 6B-C, Supporting file 2) (as enriched in DAVID gene ontology tool and IPA respectively; p < 0.05). In addition, Ingenuity Pathway Analysis (IPA)® revealed top pathways as well as the associated molecules that may be activated in dormant MDA-MB-231Br cells on soft HA hydrogels (Suppl. Fig 10, Suppl. Table 2), including glucocorticoid receptor signaling, which is known to be associated with cancer dormancy [41]. We also found that the expression pattern of specific genes/biomarker associated with cancer dormancy in our model system was largely in agreement with that reported in the literature (Table 1). Further, we observed significant upregulation of N-myc downstream regulated gene 2 (NDRG2) gene (FC = 7.59; p=0.02; q=NA) in MDA-MB-231Br cells on soft HA hydrogel (dormant) which is known to act as tumor suppressor [42], specifically through upregulation of E-Cadherin [43]. Subsequently, we observed upregulation of E-Cadherin (*CDH1*; FC = 7.74; p=0.54; q=NA) in MDA-MB-231Br cells on soft HA hydrogel (dormant) however this did not reach statistical significance. Interestingly, along with upregulation of E-cadherin (an epithelial marker [44]), we also observed a significant downregulation of vimentin (a mesenchymal marker [44]) (*VIM*; FC = -2.47; p=0.001; q=0.06) in MDA-MB-231Br cells on soft HA hydrogel (dormant). Overall, RNA-seq analysis further confirmed the dormant vs. proliferative phenotype observed in our model system.

4. Discussion

In this study, we utilized a HA hydrogel platform to model dormancy in brain metastatic breast cancer cells *in vitro*. As ECM is one of the key components of the tumor microenvironment which mediates the dormant phenotype in cancer cells, studies have recently reported on biomaterial-based *in vitro* platforms which recapitulate the key bio-physical/-chemical aspects of ECM to model cancer dormancy in the context of primary tumor [10–18,20]. However, very few studies have reported on using utilizing biomaterials-based *in vitro* platform to study breast cancer dormancy in a metastatic setting [21,23–26]. Mouse models have been utilized to study cancer dormancy at metastatic site, however, mouse models do not offer control or tunability of specific ECM properties leading to inadequate decoupling of signals provided by tumor microenvironment [2]. Amidst limited scientific advances

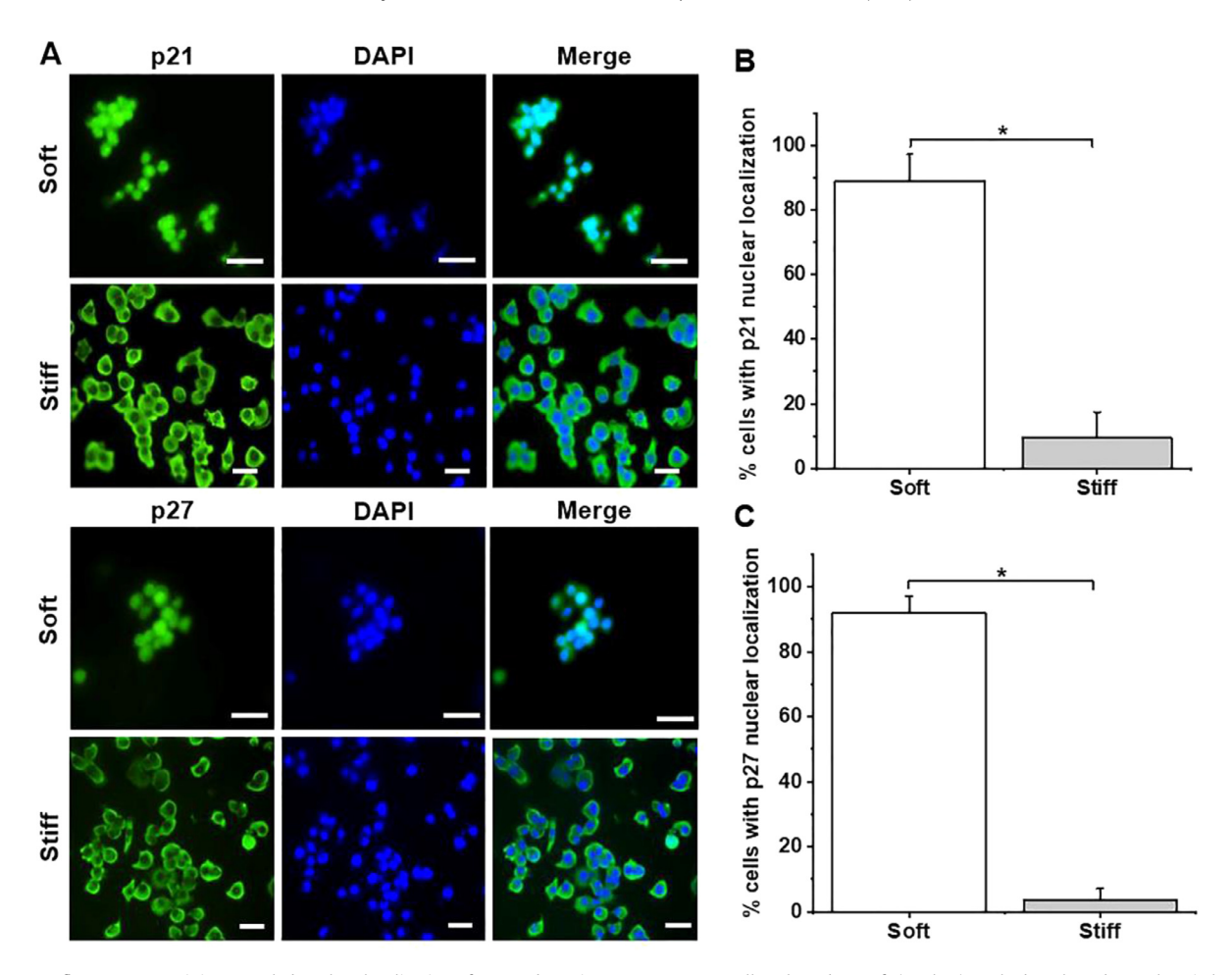


Fig. 3. Immunofluorescence staining revealed nuclear localization of p21 and p27 in MDA-MB-231Br cells cultured on soft (0.4 kPa) HA hydrogels and cytoplasmic localization on stiff (4.5 kPa) HA hydrogels. A. Representative fluorescence microscopy images of p21 (upper panel) and p27 (lower panel) staining at day 2 of MDA-MB-231Br cells cultured on soft (0.4 kPa) and stiff (4.5 kPa) HA hydrogel respectively. Green: p21 or p27; Blue: DAPI (nuclei). Scale bar = 100 µm. B. Quantification of MDA-MB-231Br cells with nuclear localization of p21 on soft (0.4 kPa) and stiff (4.5 kPa) HA hydrogel respectively. C. Quantification of MDA-MB-231Br cells with nuclear localization of p27 on soft (0.4 kPa) and stiff (4.5 kPa) HA hydrogel respectively. N = 3 replicates per condition. * indicates statistical significance (p<0.05). Error bar represents standard deviation. (For interpretation of the references to colour in this figure legend, the reader is referred to the web version of this article.)

in developing models for studying cancer dormancy, specifically in the context of metastasis, we report for the first time on an experimental *in vitro* model to study dormancy in brain metastatic breast cancer cells in a controlled setting.

We engineered mechanically soft (0.4 kPa) and stiff (4.5 kPa) HA hydrogels bracketing the normal brain (0.2-1 kPa [45]) and metastatic brain malignancy (~3.74 kPa [46]) relevant stiffness range, while maintaining similar HA composition, which allowed decoupling of the biophysical and biochemical cues. We further resorted to utilizing a 3D 'on-top' [47] approach wherein we cultured brain metastatic breast cancer cells MDA-MB-231Br and BT474Br3 on top of soft and stiff HA hydrogels. Previous studies have extensively employed EdU/Ki67-negativity as characteristic of a dormant phenotype [10,16,21,24,39]. In our system, we observed that MDA-MB-231Br cells were largely EdU and Ki67 negative when cultured on soft HA hydrogel compared to stiff HA hydrogel (Figs. 1A,B, 2A,B). A large proportion of EdU- and Ki67-negative cells indicated that the MDA-MB-231Br cells were growth arrested, indicating a dormant phenotype when cultured on soft HA hydrogels. Similar observation was made in case of BT474Br3 cells, wherein cells exhibited lowered EdU and Ki67 positivity when cultured on soft HA hydrogels compared to stiff HA hydrogel (Figs. 1C,D and 2C,D). Interestingly, previous work by Chen et al., demonstrated that high molecular weight HA promotes quiescence in bone seeking breast cancer cells MDA-MB-231BO when cultured on plates coated with basement membrane extract containing HA as characterized by low Ki67 and high p21 expression levels [48]. Herein, for the first time, we demonstrate that the biophysical cues provided by a HA hydrogel substrate drives dormancy in brain metastatic breast cancer cells, wherein culturing brain metastatic breast cancer cells on soft HA hydrogels induced a dormant phenotype whereas a stiff HA hydrogel promoted a proliferative phenotype. Further, we also demonstrated that the substrate stiffness-driven dormancy in brain metastatic breast cancer cells was reversible (Suppl. Fig. 5). One of the major differentiating factors of the presented HA hydrogel platform to model dormancy is that it induces dormancy without physical immobilization/confinement of cells (most commonly used approach to model dormancy wherein cells are encapsulated in stiff matrices [5]) while recapitulating some of the key aspects of metastatic site-specific microenvironment.

Interestingly, the magnitude of difference in the EdU and Ki67 status was more dramatic in case of MDA-MB-231Br cells when cultured on soft and stiff HA hydrogel respectively, compared to BT474Br3 cells (Figs. 1 and 2). This may be attributed to the difference in the extent of dependence of proliferation of different cell types on adhesion to the substrate. Based on the morphology of MDA-MB-231Br cells and BT474Br3 cells cultured on HA hydrogel (Suppl. Fig. 1), it is possible that the extent of dependence of proliferation on adhesion to the substrate is more pronounced in MDA-MB-231Br (sheet forming cells) compared

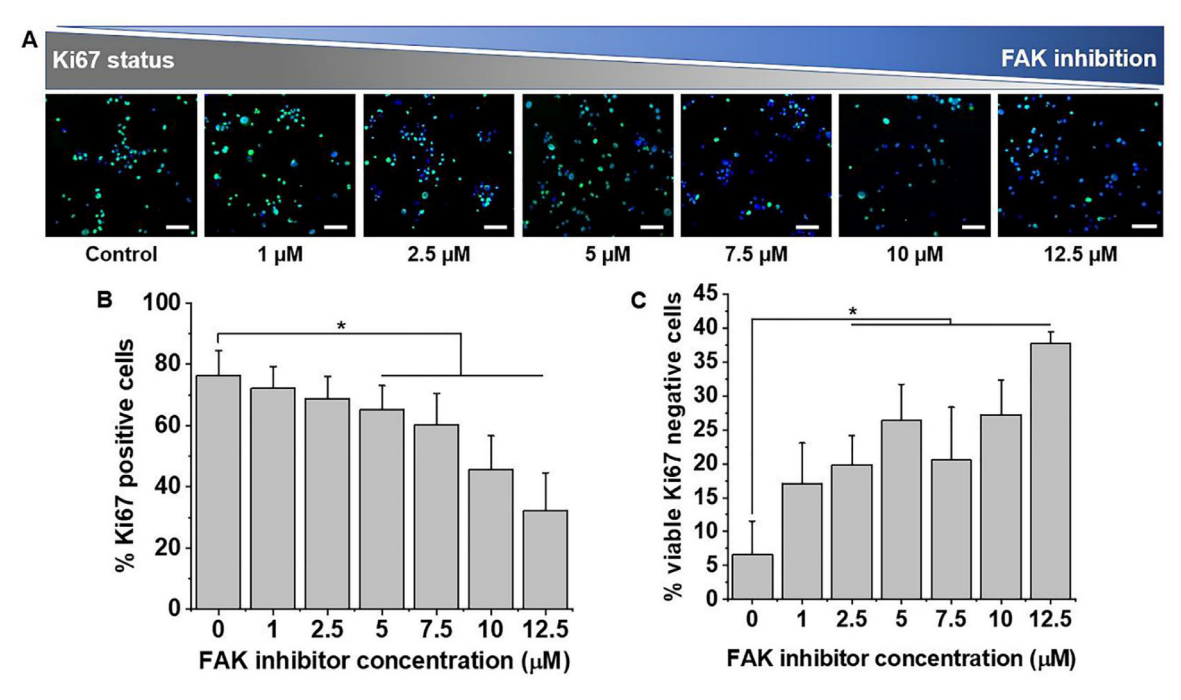


Fig. 4. FAK mediated the stiffness-based dormancy in brain metastatic breast cancer cells. Blocking FAK in proliferative MDA-MB-231Br cells cultured on stiff (4.5 kPa) HA hydrogel resulted in a partial dormant phenotype as characterized by a decrease in Ki67 positive cells and an increase in viable Ki67 negative cells with increasing FAK inhibitor concentration. A. Representative fluorescence microscopy images of Ki67 staining at day 3 of MDA-MB-231Br cells cultured on stiff HA hydrogel in the presence of varying concentrations of FAK inhibitor. Green: Ki67; Blue: DAPI (nuclei). Scale bar = 100 μ m. B. Quantification of Ki67-positive MDA-MB-231Br cells cultured on stiff HA hydrogel in presence of varying concentrations of FAK inhibitor. C. Quantification of viable Ki67-negative MDA-MB-231Br cells on stiff HA hydrogel in presence of varying concentrations of FAK inhibitor. N = 6 replicates per condition. *indicates statistical significance (p < 0.05). Error bar represents standard deviation. (For interpretation of the references to colour in this figure legend, the reader is referred to the web version of this article.)

to BT474Br3 (sphere forming cells), making MDA-MB-231Br cell proliferation more sensitive to substrate stiffness compared to BT474Br3 cells. Further, we performed immunofluorescence staining to detect phospho-FAK in MDA-MB-231Br and BT474Br3 cells on 2D TCPS, which revealed qualitatively higher expression of phospho-FAK in MDA-MB-231Br cells compared to BT474Br3 cells (Suppl. Fig. 11). These differences in inherent phospho-FAK expression levels (i.e., on 2D TCPS) may result into higher substrate (HA hydrogel) adhesion in case of MDA-MB-231Br cells resulting in a sheet like morphology compared to lower substrate adhesion in case of BT474Br3 cells resulting in sphere formation. However, further studies are needed to establish if the differences in phospho-FAK expression levels and the extent of dependence of proliferation on substrate adhesion differentially drive the morphology and dormancy in the MDA-MB-231Br and BT474Br3 cells in this model system. Nonetheless, similar observations were made by Marlow et al., wherein the magnitude of differences in the Ki67 status between dormant and proliferative breast cancer cells varied between cell lines [21]. This points to the fact that cancer cell lines differ in their genetic and biological makeup which demands for investigation into cell line specific behavior while adapting this platform to study dormancy [7].

Further, for the first time, we demonstrated the correlation between intracellular localization of cyclin dependent kinase inhibitors p21 and p27 and the dormant vs. proliferative phenotype in MDA-MB-231Br brain metastatic breast cancer cells. We observed nuclear localization of p21 and p27 in MDA-MB-231Br cells on soft HA hydrogel (dormant) contrary to the cytoplasmic localization in MDA-MB-231Br cells on stiff HA hydrogel (proliferative) (Fig. 3). p21 and p27 are known to drive dormancy in cancer cells [6,49]. Previously, studies have reported on changing intracellular localization of p21 and p27 in cancer cells [11,13,50] with nuclear localization associated with growth inhibition and cytoplasmic localization associated with tumor progression [50–55].

Herein, for the first time, we show that this process is tightly regulated by the HA hydrogel stiffness. A recent study by Liu et al. demonstrated that a stiff fibrin hydrogel restricted the growth of encapsulated melanoma cells through epigenetic upregulation of p21 and p27 leading to dormancy [18]. Taubenberger et al. also recently demonstrated the growth attenuation of breast cancer cells encapsulated within stiff PEG-heparin hydrogels along with upregulation of p21 [56]. Further, Nam et al. recently demonstrated that the fast-relaxing alginate hydrogels promote growth of encapsulated MDA-MB-231 cells through phosphatidylinositol 3-kinase (PI3K)/Akt pathway which drives cytoplasmic localization of p27, contrary to nuclear localization of p27 in growth arrested MDA-MB-231 cells encapsulated in slow-relaxing alginate hydrogels [57]. Previously, we demonstrated that blocking PI3K pathway reduced the cellular proliferation in MDA-MB-231Br cells cultured on stiff HA hydrogel whereas it did not impact the proliferation in MDA-MB-231Br cells on soft HA hydrogel, which suggests that the proliferative phenotype of MDA-MB-231Br cells on stiff HA hydrogel is partly mediated by PI3K activity [7]. Therefore, in the present study, it is plausible that activation of PI3K pathway in MDA-MB-231Br cells on stiff HA hydrogel (proliferative) drives the cytoplasmic localization of p21 and p27, whereas they exhibit nuclear localization in MDA-MB-231Br cells cultured on soft HA hydrogel (dormant) due to inadequate PI3K signaling. Taken together, we confirmed the dormant vs. proliferative phenotype observed in these cells by assessing both markers associated with proliferation (i.e., Ki67 and EdU) as well as cell cycle arrest (i.e., p21 and p27).

Previously, we demonstrated the role of FAK signaling in partly mediating the stiffness dependent proliferation of MDA-MB-231Br cells [7]. Specifically, we reported a reduction in proliferation of MDA-MB-231Br cells on stiff HA hydrogels following FAK inhibition [7]. In the present study, we explored the role of FAK in the stiffness mediated dormancy in MDA-MB-231Br brain metastatic breast cancer cells. We observed that blocking FAK signaling in

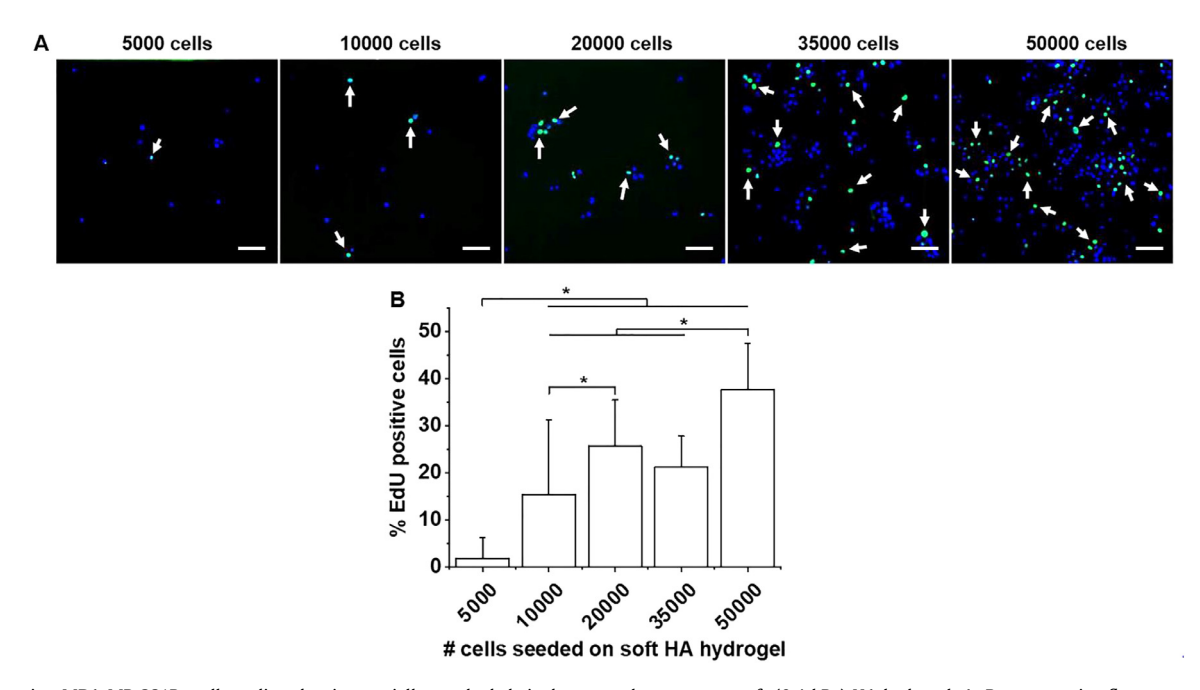


Fig. 5. Increasing MDA-MB-231Br cell seeding density partially revoked their dormant phenotype on soft (0.4 kPa) HA hydrogel. A. Representative fluorescence microscopy images of EdU staining (white arrowheads) at day 3 of MDA-MB-231Br cells cultured on soft HA hydrogel at varying cell seeding densities of 5000, 10,000, 20,000, 35,000 and 50,000 cells per hydrogel respectively. Green: EdU; Blue: DAPI (nuclei). Scale bar = 100 μm. B. Quantification of EdU positive MDA-MB-231Br cells cultured on soft HA hydrogel at varying cell seeding densities of 5000, 10,000, 20,000, 35,000 and 50,000 cells per hydrogel respectively. N = 6 replicates per condition. * indicates statistical significance (p<0.05). Error bar represents standard deviation. (For interpretation of the references to colour in this figure legend, the reader is referred to the web version of this article.)

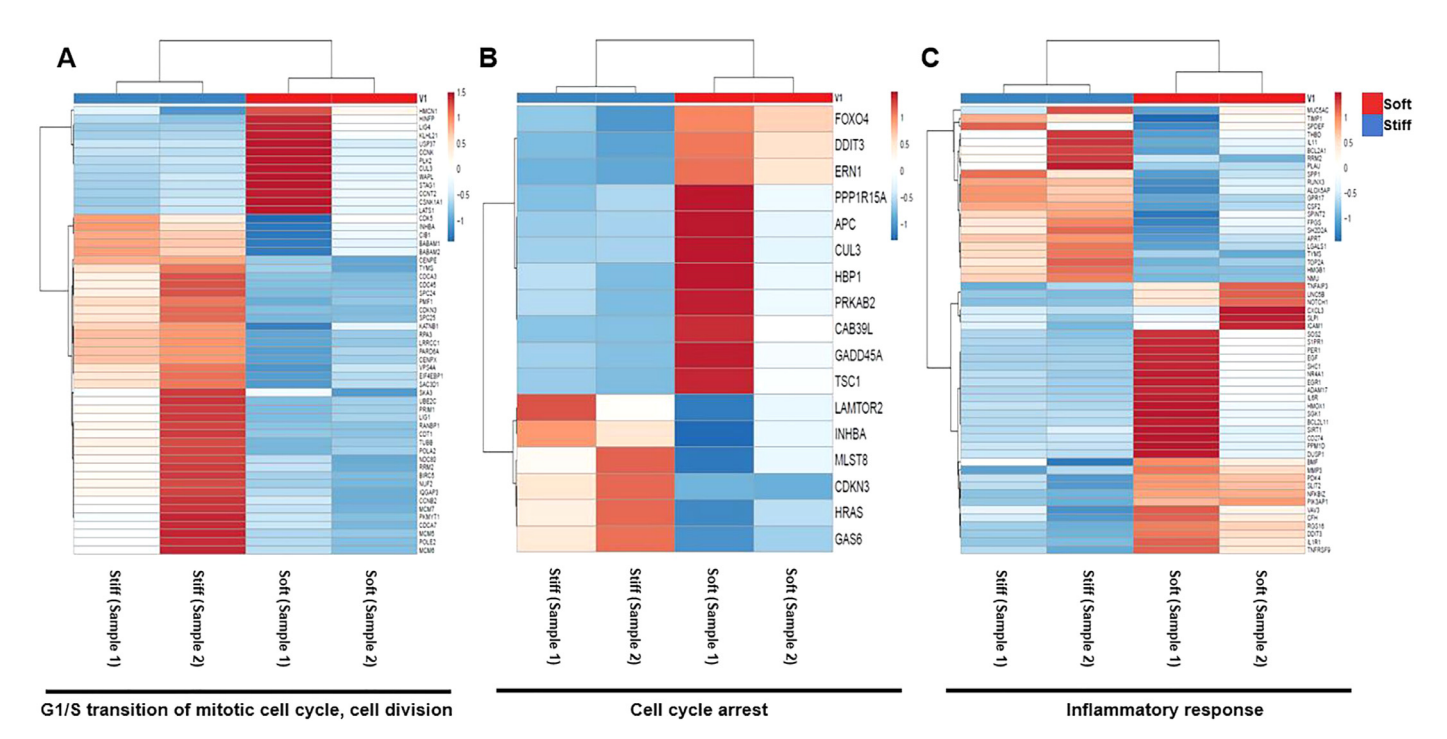


Fig. 6. RNA-seq. analysis revealed differentially regulated genes in dormant MDA-MB-231Br cells cultured on soft (0.4 kPa) HA hydrogel compared to proliferative MDA-MB-231Br cells on stiff (4.5 kPa) HA hydrogel. Gene classification was performed using DAVID gene ontology tool and Ingenuity Pathway Analysis, and heatmaps were generated using ClustVis. A. Genes associated with G1/S transition of mitotic cell cycle and cell division were largely downregulated in dormant MDA-MB-231Br cells on soft HA hydrogel. B. Genes associated with cell cycle arrest were largely upregulated in dormant MDA-MB-231Br cells on soft HA hydrogel. C. Genes associated with inflammatory response were largely upregulated in dormant MDA-MB-231Br cells on soft HA hydrogel. Quality of 1394 differentially regulated genes, 121 genes are depicted in the presented categories. Genes having a fold change of at least ± 2 and showing a significant statistical difference (compared to MDA-MB-231Br cells on stiff HA hydrogel) (p < 0.05) were considered. N = 2 RNA seq. runs; $n \ge 5$ hydrogels per run.

Table 1 Expression pattern of specific genes/biomarker associated with cancer dormancy as reported in the literature and in dormant MDA-MB-231Br cells on soft HA hydrogel. Genes with FC cut-off of ± 2 and/or p < 0.05 are included in the table. Positive FC value indicates upregulation and negative FC value indicates downregulation.

Sr. No.	Gene/Biomarker	Ref.	Fold Change (compared to MDA-MB-231Br on stiff HA hydrogel)	p-value	q-value
Genes/b	iomarkers largely reported to	o be upregu	lated during cancer dormancy in the liter	ature	
1	TGFBR3	[6]	2.42	0.0016	0.0833
2	TNFRSF1B	[6]	2.43	0.0534	0.3988
3	TNFRSF9	[6]	3.96	0.0457	0.3798
4	TNFRSF10C	[6]	2.02	0.0803	0.4599
5	TNFRSF10D	[6]	2.70	0.0004	0.0367
6	HIST1H2BK (or H2BC12)	[71]	5.99	9.05E-09	7.97E-0
7	IGFBP5	[71]	6.13	0.5902	-NA-
8	MMP2	[71]	11.64	0.3976	-NA-
9	CFH	[72]	2.23	0.0058	0.1506
10	GADD45B	[72]	4.93	2.72E-05	0.0072
11	ASL	[72]	-2.09	0.0554	0.4029
12	LOXL1	[72]	-4.10	0.0004	0.0368
13	DEC1	[73]	7.74	0.5422	-NA-
14	HBP1	[22]	3.79	1.21E-05	0.0038
15	CDH1	[65–67]	7.74	0.5422	-NA-
16	LIFR	[74]	2.04	0.0251	0.2929
17	EGR1	[68]	3.44	3.78E-05	0.0092
18	TNF	[68]	11.38	0.0325	-NA-
19	TNFAIP3	[68]	3.80	0.0005	0.0423
20	PTGS2	[68]	2.24	0.0515	0.3924
21	HIST2H2BE (or H2BC21)	[68]	6.81	3.51E-05	0.0086
22	SOX2	[19,75]	22.83	0.1453	-NA-
23	NFKBIZ	[68]	3.31	6.27E-05	0.0119
24	CDKN1A (p21)	[6]	1.69	0.0558	0.4036
Genes/b			gulated during cancer dormancy in the lit		
1	MKI67	[24,76]	-2.01	0.0206	0.2635
2	CDKN3	[71]	-2.60	0.0006	0.0492
3	DTYMK	[71]	-2.61	0.0004	0.0422
4	ESM1	[71]	-3.92	0.5813	-NA-
5	FOXD1	[71]	-4.57	0.6566	-NA-
6	TK1	[71]	-2.49	0.0018	0.0877
7	PLAU (uPA)	[40]	-3.50	2.25E-05	0.0063
8	ASNS	[71]	2.20	0.0052	0.1416
9	ATF3	[71]	9.40	2.85E-10	4.46E-0

MDA-MB-231Br cells on stiff HA hydrogel (proliferative) led to an induction of dormant phenotype as indicated by FAK inhibitor 14 dose-dependent increase in the proportion of viable Ki67-negative cells (Fig. 4). Our observations are in line with a previous study by Aguirre Ghiso, wherein inhibition of FAK signaling led to dormancy in HEp3 human carcinoma cells [40]. Further, Schrader et al. also demonstrated lowered FAK activity in dormant Huh7 and HepG2 cells cultured on top of soft collagen-I coated polyacrylamide hydrogels compared to proliferative cells on stiff hydrogels [58]. In addition, they reported a significant reduction in proliferation in Huh7 and HepG2 hepatocellular carcinoma cells cultured on top of stiff collagen-I coated polyacrylamide hydrogels following FAK inhibition [58]. Herein, we established for the first time, the role of FAK in partly mediating the stiffness-based dormancy in MDA-MB-231Br brain metastatic breast cancer cells utilizing a HA hydrogel platform.

Interestingly, we also observed that increasing the initial cell seeding density of MDA-MB-231Br cells on soft HA hydrogel partly revokes the dormant phenotype as indicated by increased proportion of EdU positive cells (Fig. 5). This suggests that, in this model, cell seeding density indeed overrides the biophysical cues provided by soft HA hydrogel, which drive dormancy in the first place. Our observations are in line with those recently reported by Venugopal et al., wherein they observed that increasing the cell density on soft poly-acrylamide gels led to cell spreading and revoked cell cycle arrest induced by soft substrate thereby promoting cell cycle progression in human mesenchymal stem cells [59]. They attributed this result to the local strain-stiffening of soft substrate due to high cell seeding density which promotes cellular processes [59]. In the context of cell-biomaterial interactions underlying this

dormancy model; through the varying cell seeding density experiment, we demonstrated that altering the cell seeding density indeed impacts the phenotype conferred by the mechanical cues from the biomaterial. This aspect should be taken into consideration when adapting this dormancy model. Further, in an in vivo setting, studies have indicated that the presence of circulating tumor cells (CTC) clusters (also known as 'Tumor Microemboli') is associated with a more aggressive metastatic potential particularly in breast, prostate and small-cell lung cancer compared to single CTCs [60-64]. It is plausible that enhanced cell-cell interactions in CTC clusters may mask metastatic cells from the adversities posed by foreign microenvironment (or foreign ECM in this case), resulting in early dormant to emergent switch and early establishment of metastasis. Therefore, our observation that increasing cell seeding density overrides the impact of soft HA hydrogel (matrix) resulting in a proliferative phenotype, supports the previously established in vivo observation pertaining to the presence of CTC clusters and their increased metastatic potential. This observation also suggests that the interplay between tumor cell-tumor cell and tumor cell-matrix interactions may govern dormancy at the metastatic

Whole transcriptome RNA sequencing further confirmed the dormant phenotype of MDA-MB-231Br brain metastatic breast cancer cells on soft HA hydrogels (Fig. 6A,B, Table 1). We identified multiple genes/biomarkers positively associated with cancer dormancy as reported in the literature to be upregulated in MDA-MB-231Br cells on soft HA hydrogel (dormant) (Table 1). However, there were some genes whose expression pattern was discordant with that reported in the literature. For example, ASL (FC = -2.09; p = 0.05; q = 0.40) and LOXL1 (FC = -4.105;

p=0.0004; q=0.03) genes were significantly downregulated and ASNS (FC = 2.20; p=0.005; q=0.14) and ATF3 (FC = 9.4; p=2.85E-10; q=4.46E-07) significantly upregulated in MDA-MB-231Br cells on soft HA hydrogel (dormant) contrary to the established notion (Table 1). These discrepancies necessitate further investigation into metastatic site-specific expression pattern of genes associated with dormancy in metastatic breast cancer cells.

Through RNA sequencing, we also found that Ki67 (MKI67; FC = -2.01; p = 0.02; q = 0.26) was significantly downregulated in MDA-MB-231Br cells on soft HA hydrogel (dormant) compared to the proliferative cells on stiff HA hydrogel (Table 1), consistent with our results obtained through immunofluorescence staining (Fig. 2A, B). Further, we also observed significant upregulation of p21 (CDKN1A; FC = 1.69; p = 0.05; q = 0.40) (Table 1) in dormant MDA-MB-231Br cells on soft HA hydrogels compared to the proliferative cells on stiff HA hydrogel, however, p27 (CDKN1B; FC = 1.26; p = 0.41; q = 0.77) was not differentially regulated. This suggests that, in the case of p27, it might be solely the intracellular localization at the protein level and not the respective gene expression level that is involved in dormancy. Further, we noted significant upregulation of N-myc downstream regulated gene 2 (NDRG2) (FC = 7.59; p = 0.02; q=NA) in MDA-MB-231Br cells on soft HA hydrogel (dormant), which belongs to the same family as NDRG1, which is implicated in cancer dormancy [6,49]. NDRG2 has been known to act as a tumor suppressor gene and its expression levels have been positively correlated with improved prognosis [42], however, its role in cancer dormancy still remains unknown. Kim et al. demonstrated that NDRG2 acts as tumor suppressor through upregulation of E-cadherin [43]. Interestingly, previous literature suggests that the increase in E-cadherin adhesions as a result of mesenchymal to epithelial reverse transition (MErT) may result in a dormant phenotype at the metastatic site [65-67], however, it should be also noted that the specific phenotype of dormant cancer cells remains unknown [58]. In the present study, we did note an upregulation of E-Cadherin (an epithelial marker [44]) (CDH1; FC = 7.74; p = 0.54; q=NA) followed by significant downregulation of vimentin (a mesenchymal marker [44]) (VIM; FC = -2.47; p = 0.001; q = 0.06) in MDA-MB-231Br cells on soft HA hydrogel (dormant), however, further investigations are needed to ascertain if the dormancy in MDA-MB-231Br cells on soft HA hydrogels is a result of MErT. In addition, we observed an increased expression of multiple genes associated with inflammatory response in dormant MDA-MB-231Br cells on soft HA hydrogel (Fig. 6C). Previously, Bartosh et al. have reported increased expression levels of factors associated with inflammatory response in dormant MDA-MB-231 cells following cannibalization of mesenchymal stem cells (MSCs) by MDA-MB-231 cells [68]. This may be attributed to senescence associated secretory phenotype which is plethora of pro-inflammatory factors through which the dormant cancer cells engage in a crosstalk with neighboring cells in the process of remodeling the microenvironment [68-70].

Some limitations of this dormancy model that should be taken into consideration are as follows: (i) As the HA hydrogel platform was engineered to contain only one particular RGD density, future investigations should consider the impact of varying RGD density on the dormancy-related responses in this system. (ii) As this model utilizes a '3D on top' approach; the complexity of this system could be further increased via incorporation of additional microenvironmental components or a 3D encapsulation approach, to closely model dormancy with additional physiological relevance. Overall, in the present study, we demonstrated a biomimetic HA hydrogel platform to model dormancy in brain metastatic breast cancer cells via exploiting the bio-physical cues provided by the substrate while recapitulating the metastatic site-specific microenvironment.

5. Conclusions

Here, we successfully utilized a HA hydrogel platform to develop an in vitro metastatic site-specific model of cancer dormancy in brain metastatic breast cancer cells via exploiting the bio-physical cues provided by the substrate. We observed that the brain metastatic breast cancer cells exhibit a dormant phenotype when cultured on top of soft HA hydrogel whereas they exhibit a proliferative phenotype when cultured on stiff HA hydrogel as noted by their EdU and Ki67 status. For the first time, we demonstrated that the cyclin dependent kinase inhibitors p21 and p27 exhibit a nuclear localization in dormant MDA-MB-231Br brain metastatic breast cancer cells on soft HA hydrogels contrary to their cytoplasmic localization in proliferative MDA-MB-231Br cells on stiff HA hydrogels. Further, we established that the HA hydrogel stiffness driven dormancy was reversible and was, in part, mediated by FAK signaling. We also demonstrated that the dormant phenotype of MDA-MB-231Br cells on soft HA hydrogels is impacted by the initial cell seeding density wherein higher initial cell seeding densities partly revoke dormancy. Whole transcriptome RNA sequencing revealed that the expression pattern of specific genes/biomarker associated with cancer dormancy in MDA-MB-231Br cells on soft HA hydrogels was largely in agreement with that reported in the literature, further confirming their dormant phenotype. Such a biomimetic HA hydrogel platform could be utilized to further our understanding of dormancy associated with breast cancer brain metastasis through further investigations into cell-material interactions. In future, such an in vitro platform can be adapted to serve as a high throughput anti-metastatic drug screen to specifically target dormant cancer cells.

Declaration of Competing Interest

The authors declare no conflict of interest.

Acknowledgements

This work was supported by a National Science Foundation CA-REER award (CBET 1749837, to S.R.), University of Alabama Research Grants Committee (RG14751, to S.R.), and, in part, by the Breast Cancer Research Foundation of Alabama (to S.R. and L.S.). The authors also acknowledge financial support through the Alabama EPSCoR Graduate Research Fellowship (to A.N.) and The University of Alabama Graduate Council Fellowship (to A.N.). The authors would like to thank Pinaki Nakod (The University of Alabama) for experimental assistance with RNA extraction and Dr. Michael Crowley (Genomic Science Core Laboratories, University of Alabama at Birmingham) for experimental assistance with RNA-seq.

Supplementary materials

Supplementary material associated with this article can be found, in the online version, at doi:10.1016/j.actbio.2020.02.039.

References

- A.A. Narkhede, L.A. Shevde, S.S. Rao, Biomimetic strategies to recapitulate organ specific microenvironments for studying breast cancer metastasis, Int. J. Cancer 141 (2017) 1091–1109.
- [2] S.S. Rao, R.V. Kondapaneni, A.A. Narkhede, Bioengineered models to study tumor dormancy, J. Biol. Eng. 13 (2019) 3.
- [3] J.A. Aguirre-Ghiso, P. Bragado, M.S. Sosa, Metastasis awakening: targeting dormant cancer, Nat. Med. 19 (2013) 276–277.
- [4] C.A. Klein, Framework models of tumor dormancy from patient-derived observations, Curr. Opin. Genet. Dev. 21 (2011) 42–49.
- [5] S. Pradhan, J.L. Sperduto, C.J. Farino, J.H. Slater, Engineered in vitro models of tumor dormancy and reactivation, J. Biol. Eng. 12 (2018) 37.

- [6] M.S. Sosa, P. Bragado, J.A. Aguirre-Ghiso, Mechanisms of disseminated cancer cell dormancy: an awakening field, Nat. Rev. Cancer 14 (2014) 611-622.
- [7] A.A. Narkhede, J.H. Crenshaw, R.M. Manning, S.S. Rao, The influence of matrix stiffness on the behavior of brain metastatic breast cancer cells in a biomimetic hyaluronic acid hydrogel platform, J. Biomed. Mater. Res. A 106 (2018) 1832-1841.
- [8] I. Witzel, L. Oliveira-Ferrer, K. Pantel, V. Müller, H. Wikman, Breast cancer brain metastases: biology and new clinical perspectives, Breast Cancer Res. 18 (2016) 8.
- [9] H. Endo, M. Inoue, Dormancy in cancer, Cancer Sci. 110 (2019) 474–480.
 [10] S. Pradhan, J.H. Slater, Tunable hydrogels for controlling phenotypic cancer cell states to model breast cancer dormancy and reactivation, Biomaterials 215 (2019) 119177
- [11] D. Barkan, H. Kleinman, J.L. Simmons, H. Asmussen, A.K. Kamaraju, M.J. Hoenorhoff, Z.-Y. Liu, S.V. Costes, E.H. Cho, S. Lockett, C. Khanna, A.F. Chambers, J.E. Green, Inhibition of metastatic outgrowth from single dormant tumor cells by targeting the cytoskeleton, Cancer Res 68 (2008) 6241-6250
- [12] D. Barkan, J.E. Green, An in vitro system to study tumor dormancy and the switch to metastatic growth, J. Vis. Exp. (2011) e2914.
- [13] L.H. El Touny, A. Vieira, A. Mendoza, C. Khanna, M.J. Hoenerhoff, J.E. Green, Combined SFK/MEK inhibition prevents metastatic outgrowth of dormant tumor cells, J. Clin. Invest. 124 (2014) 156-168.
- [14] D. Barkan, L.H. El Touny, A.M. Michalowski, J.A. Smith, I. Chu, A.S. Davis, J.D. Webster, S. Hoover, R.M. Simpson, J. Gauldie, J.E. Green, Metastatic growth from dormant cells induced by a col-I-enriched fibrotic environment, Cancer Res 70 (2010) 5706-5716.
- [15] K. Guiro, S.A. Patel, S.J. Greco, P. Rameshwar, T.L. Arinzeh, Investigating breast cancer cell behavior using tissue engineering scaffolds, PLoS ONE 10 (2015) e0118724.
- [16] C.M. Ghajar, H. Peinado, H. Mori, I.R. Matei, K.J. Evason, H. Brazier, D. Almeida, A. Koller, K.A. Hajjar, D.Y.R. Stainier, E.I. Chen, D. Lyden, M.J. Bissell, The perivascular niche regulates breast Tumour dormancy, Nat. Cell Biol. 15 (2013) 807-817.
- [17] J.Y. Fang, S.-.J. Tan, Y.-.C. Wu, Z. Yang, B.X. Hoang, B. Han, From competency to dormancy: a 3D model to study cancer cells and drug responsiveness, J. Transl. Med. 14 (2016) 38.
- [18] Y. Liu, J. Lv, X. Liang, X. Yin, L. Zhang, D. Chen, X. Jin, R. Fiskesund, K. Tang, J. Ma, H. Zhang, W. Dong, S. Mo, T. Zhang, F. Cheng, Y. Zhou, J. Xie, N. Wang, B. Huang, Fibrin stiffness mediates dormancy of tumor-repopulating cells via a CDC42-driven TET2 epigenetic program, Cancer Res 78 (2018) 3926-3937
- [19] Q. Jia, F. Yang, W. Huang, Y. Zhang, B. Bao, K. Li, F. Wei, C. Zhang, H. Jia, Low levels of sox2 are required for melanoma tumor-repopulating cell dormancy, Theranostics 9 (2019) 424-435.
- [20] T.S. Pavan Grandhi, T. Potta, R. Nitiyanandan, I. Deshpande, K. Rege, Chemomechanically engineered 3D organotypic platforms of bladder cancer dormancy and reactivation, Biomaterials 142 (2017) 171-185.
- [21] R. Marlow, G. Honeth, S. Lombardi, M. Cariati, S.M. Hessey, A. Pipili, V. Mariotti, B. Buchupalli, K. Foster, D. Bonnet, A. Grigoriadis, A. Purushotham, A. Tutt, G. Dontu, A novel model of dormancy for bone metastatic breast cancer cells, Cancer Res. 73 (2013) 6886-6899.
- [22] J. McGrath, L. Panzica, R. Ransom, H.G. Withers, I.H. Gelman, Identification of genes regulating breast cancer dormancy in 3D bone endosteal niche cultures, Mol. Cancer Res. 17 (2019) 860-869.
- [23] D.M. Sosnoski, R.J. Norgard, C.D. Grove, S.J. Foster, A.M. Mastro, Dormancy and growth of metastatic breast cancer cells in a bone-like microenvironment, Clin. Exp. Metastasis 32 (2015) 335-344.
- [24] S.E. Wheeler, A.M. Clark, D.P. Taylor, C.L. Young, V.C. Pillai, D.B. Stolz, R. Venkataramanan, D. Lauffenburger, L. Griffith, A. Wells, Spontaneous dormancy of metastatic breast cancer cells in an all human liver microphysiologic system, Br. J. Cancer 111 (2014) 2342-2350.
- [25] D.P. Taylor, A. Clark, S. Wheeler, A. Wells, Hepatic nonparenchymal cells drive metastatic breast cancer outgrowth and partial epithelial to mesenchymal transition, Breast Cancer Res. Treat. 144 (2014) 551-560.
- [26] A.M. Clark, S.E. Wheeler, C.L. Young, L. Stockdale, J. Shepard Neiman, W. Zhao, D.B. Stolz, R. Venkataramanan, D. Lauffenburger, L. Griffith, A. Wells, A liver microphysiological system of tumor cell dormancy and inflammatory responsiveness is affected by scaffold properties, Lab Chip 17 (2017) 156-168.
- [27] G.N. Naumov, I.C. MacDonald, P.M. Weinmeister, N. Kerkvliet, K.V. Nadkarni, S.M. Wilson, V.L. Morris, A.C. Groom, A.F. Chambers, Persistence of solitary mammary carcinoma cells in a secondary site: a possible contributor to dormancy, Cancer Res 62 (2002) 2162-2168.
- [28] C. Heyn, J.A. Ronald, S.S. Ramadan, J.A. Snir, A.M. Barry, L.T. MacKenzie, D.J. Mikulis, D. Palmieri, J.L. Bronder, P.S. Steeg, T. Yoneda, I.C. MacDonald, A.F. Chambers, B.K. Rutt, P.J. Foster, In vivo MRI of cancer cell fate at the single-cell level in a mouse model of breast cancer metastasis to the brain, Magn. Reson. Med. 56 (2006) 1001-1010.
- [29] L. Jadin, S. Pastorino, R. Symons, N. Nomura, P. Jiang, T. Juarez, M. Makale, S. Kesari, Hyaluronan expression in primary and secondary brain tumors, Ann. Transl. Med. 3 (2015) 80.
- [30] K.J. Wolf, S. Kumar, Hyaluronic acid: incorporating the bio into the material, ACS Biomater. Sci. Eng. 5 (2019) 3753–3765.
 [31] B. Ananthanarayanan, Y. Kim, S. Kumar, Elucidating the mechanobiology of ma-
- lignant brain tumors using a brain matrix-mimetic hyaluronic acid hydrogel platform, Biomaterials 32 (2011) 7913-7923.

- [32] S.M. Saldana, H.-.H. Lee, F.J. Lowery, Y.B. Khotskaya, W. Xia, C. Zhang, S.-.S. Chang, C.-.K. Chou, P.S. Steeg, D. Yu, M.-.C. Hung, Inhibition of type i insulin-like growth factor receptor signaling attenuates the development of breast cancer brain metastasis, PLoS ONE 8 (2013) e73406-e73406.
- [33] M. Sobecki, K. Mrouj, J. Colinge, F. Gerbe, P. Jay, L. Krasinska, V. Dulic, D. Fisher, Cell-Cycle regulation accounts for variability in ki-67 expression levels, Cancer Res 77 (2017) 2722-2734.
- [34] I.L. Townson, A.F. Chambers, Dormancy of solitary metastatic cells, Cell Cycle 5 (2006) 1744-1750.
- [35] A. Dobin, C.A. Davis, F. Schlesinger, J. Drenkow, C. Zaleski, S. Jha, P. Batut, M. Chaisson, T.R. Gingeras, STAR: ultrafast universal RNA-seq aligner, Bioinformatics 29 (2012) 15-21.
- [36] S. Anders, P.T. Pyl, W. Huber, HTSeq-a python framework to work with high--throughput sequencing data, Bioinformatics 31 (2015) 166–169.
- [37] M.I. Love, W. Huber, S. Anders, Moderated estimation of fold change and dispersion for RNA-seq data with DESeq2, Genome Biol. 15 (2014) 550.
- T. Metsalu, J. Vilo, ClustVis: a web tool for visualizing clustering of multivariate data using principal component analysis and heatmap, Nucleic Acids Res. 43 (2015) W566-W570.
- [39] A.M. Clark, M.P. Kumar, S.E. Wheeler, C.L. Young, R. Venkataramanan, D.B. Stolz, L.G. Griffith, D.A. Lauffenburger, A. Wells, A model of dormant-emergent metastatic breast cancer progression enabling exploration of biomarker signatures, Mol. Cell Proteomics 17 (2018) 619-630.
- [40] J.A. Aguirre Ghiso, Inhibition of fak signaling activated by urokinase receptor induces dormancy in human carcinoma cells in vivo, Oncogene 21 (2002) 2513-2524
- [41] S. Prekovic, K. Schuurman, A.G. Manjón, M. Buijs, I.M. Peralta, M.D. Wellenstein, S. Yavuz, A. Barrera, K. Monkhorst, A. Huber, B. Morris, C. Lieftink, J. Silva, B. Győrffy, L. Hoekman, B. van den Broek, H. Teunissen, T. Reddy, W. Faller, R. Beijersbergen, J. Jonkers, M. Altelaar, K.E. de Visser, E. de Wit, R. Medema, W. Zwart, Glucocorticoids regulate cancer cell dormancy, bioRxiv (2019) 750406, doi:https://doi.org/10.1101/750406.
- [42] A. Lorentzen, R.H. Lewinsky, J. Bornholdt, L.K. Vogel, C. Mitchelmore, Expression profile of the N-myc downstream regulated gene 2 (NDRG2) in human cancers with focus on breast cancer, BMC Cancer 11 (2011) 14.
- [43] Y.J. Kim, H.B. Kang, H.S. Yim, J.H. Kim, J.W. Kim, NDRG2 positively regulates E-cadherin expression and prolongs overall survival in colon cancer patients, Oncol. Rep. 30 (2013) 1890-1898.
- [44] M. Zeisberg, E.G. Neilson, Biomarkers for epithelial-mesenchymal transitions, J. Clin. Invest. 119 (2009) 1429-1437.
- S.S. Rao, J. DeJesus, A.R. Short, J.J. Otero, A. Sarkar, J.O. Winter, Glioblastoma behaviors in three-dimensional collagen-hyaluronan composite hydrogels, ACS Appl. Mater. Interfaces 5 (2013) 9276-9284.
- [46] Y. Jamin, J.K. Boult, J. Li, S. Popov, P. Garteiser, J.L. Ulloa, C. Cummings, G. Box, S.A. Eccles, C. Jones, Exploring the biomechanical properties of brain malignancies and their pathologic determinants in vivo with magnetic resonance elastography, Cancer Res 75 (2015) 1216-1224.
- [47] G.Y. Lee, P.A. Kenny, E.H. Lee, M.J. Bissell, Three-dimensional culture models of normal and malignant breast epithelial cells, Nat. Methods 4 (2007) 359-365.
- [48] X. Chen, Y. Du, Y. Liu, Y. He, G. Zhang, C. Yang, F. Gao, Hyaluronan arrests human breast cancer cell growth by prolonging the G0/G1 phase of the cell cycle, Acta Biochim. Biophys. Sin. 50 (2018) 1181-1189.
- [49] X.-.L. Gao, M. Zhang, Y.-.L. Tang, X.-.H. Liang, Cancer cell dormancy: mechanisms and implications of cancer recurrence and metastasis, Onco. Targets Ther. 10 (2017) 5219-5228.
- [50] A.J. Vincent, S. Ren, L.G. Harris, D.J. Devine, R.S. Samant, O. Fodstad, .A. Shevde, Cytoplasmic translocation of p21 mediates NUPR1-induced chemoresistance: NUPR1 and p21 in chemoresistance, FEBS Lett. 586 (2012)
- [51] M. Asada, T. Yamada, H. Ichijo, D. Delia, K. Miyazono, K. Fukumuro, S. Mizutani, Apoptosis inhibitory activity of cytoplasmic p21Cip1/WAF1 in monocytic differentiation, EMBO J. 18 (1999) 1223-1234.
- [52] M.V. Blagosklonny, Are p27 and p21 cytoplasmic oncoproteins? Cell Cycle 1 (2002) 391-393.
- [53] J.W. Harper, S.J. Elledge, K. Keyomarsi, B. Dynlacht, L.H. Tsai, P. Zhang, S. Dobrowolski, C. Bai, L. Connell-Crowley, E. Swindell, Inhibition of cyclin-dependent kinases by p21, Mol. Biol. Cell 6 (1995) 387-400.
- [54] H. Flores-Rozas, Z. Kelman, F.B. Dean, Z.Q. Pan, J.W. Harper, S.J. Elledge, M. Donnell, J. Hurwitz, Cdk-interacting protein 1 directly binds with proliferating cell nuclear antigen and inhibits DNA replication catalyzed by the DNA polymerase delta holoenzyme, Proc. Natl. Acad. Sci. 91 (1994) 8655-8659.
- [55] J. Zhan, J.B. Easton, S. Huang, A. Mishra, L. Xiao, E.R. Lacy, R.W. Kriwacki, P.J. Houghton, Negative regulation of ASK1 by p21Cip1 involves a small domain that includes serine 98 that is phosphorylated by ASK1 in vivo, Mol. Cell Biol. 27 (2007) 3530-3541.
- [56] A.V. Taubenberger, S. Girardo, N. Träber, E. Fischer-Friedrich, M. Kräter, K. Wagner, T. Kurth, I. Richter, B. Haller, M. Binner, D. Hahn, U. Freudenberg, C. Werner, J. Guck, 3D Microenvironment stiffness regulates tumor spheroid growth and mechanics via p21 and Rock, Adv. Biosys. 3 (2019) 1900128.
- [57] S. Nam, V.K. Gupta, H.-p. Lee, J.Y. Lee, K.M. Wisdom, S. Varma, E.M. Flaum, C. Davis, R.B. West, O. Chaudhuri, Cell cycle progression in confining microenvironments is regulated by a growth-responsive TRPV4-PI3K/Akt-p27Kip1 signaling axis, Sci. Adv. 5 (2019) eaaw6171.
- [58] J. Schrader, T.T. Gordon-Walker, R.L. Aucott, M. van Deemter, A. Quaas, S. Walsh, D. Benten, S.J. Forbes, R.G. Wells, J.P Iredale, Matrix stiffness mod-

- ulates proliferation, chemotherapeutic response, and dormancy in hepatocellular carcinoma cells, Hepatology 53 (2011) 1192–1205.
- [59] B. Venugopal, P. Mogha, J. Dhawan, A. Majumder, Cell density overrides the effect of substrate stiffness on human mesenchymal stem cells' morphology and proliferation, Biomater. Sci. 6 (2018) 1109–1119.
- [60] N. Aceto, A. Bardia, D.T. Miyamoto, M.C. Donaldson, B.S. Wittner, J.A. Spencer, M. Yu, A. Pely, A. Engstrom, H. Zhu, B.W. Brannigan, R. Kapur, S.L. Stott, T. Shioda, S. Ramaswamy, D.T. Ting, C.P. Lin, M. Toner, D.A. Haber, S. Maheswaran, Circulating tumor cell clusters are oligoclonal precursors of breast cancer metastasis, Cell 158 (2014) 1110–1122.
- [61] J.M. Hou, M.G. Krebs, L. Lancashire, R. Sloane, A. Backen, R.K. Swain, L.J. Priest, A. Greystoke, C. Zhou, K. Morris, T. Ward, F.H. Blackhall, C. Dive, Clinical significance and molecular characteristics of circulating tumor cells and circulating tumor microemboli in patients with small-cell lung cancer, J. Clin. Oncol. 30 (2012) 525–532.
- [62] Z. Ahmed, S. Gravel, Intratumor heterogeneity and circulating tumor cell clusters, Mol. Biol. Evol. 35 (2017) 2135–2144.
- [63] V.C. Ramani, C.A. Lemaire, M. Triboulet, K.M. Casey, K. Heirich, C. Renier, J.G. Vilches-Moure, R. Gupta, A.M. Razmara, H. Zhang, G.W. Sledge, E. Sollier, S.S. Jeffrey, Investigating circulating tumor cells and distant metastases in patient-derived orthotopic xenograft models of triple-negative breast cancer, Breast Cancer Res 21 (2019) 98.
- [64] A.N. May, B.D. Crawford, A.M. Nedelcu, In vitro model-systems to understand the biology and clinical significance of circulating tumor cell clusters, Front. Oncol. 8 (2018) 63.
- [65] A. Wells, C. Yates, C.R. Shepard, E-cadherin as an indicator of mesenchymal to epithelial reverting transitions during the metastatic seeding of disseminated carcinomas, Clin. Exp. Metastasis 25 (2008) 621–628.
- [66] M.K. Wendt, M.A. Taylor, B.J. Schiemann, W.P. Schiemann, Down-regulation of epithelial cadherin is required to initiate metastatic outgrowth of breast cancer, Mol. Biol. Cell 22 (2011) 2423–2435.
- [67] B. Ma, A. Wells, A.M. Clark, The pan-therapeutic resistance of disseminated tumor cells: role of phenotypic plasticity and the metastatic microenvironment, Semin. Cancer Biol. (2019).

- [68] T.J. Bartosh, M. Ullah, S. Zeitouni, J. Beaver, D.J. Prockop, Cancer cells enter dormancy after cannibalizing mesenchymal stem/stromal cells (MSCs), Proc. Natl. Acad. Sci. 113 (2016) E6447–E6456.
- [69] J.-P. Coppé, P.-Y. Desprez, A. Krtolica, J. Campisi, The senescence-associated secretory phenotype: the dark side of tumor suppression, Annu. Rev. Pathol. 5 (2010) 99–118.
- [70] P.A. Perez-Mancera, A.R. Young, M. Narita, Inside and out: the activities of senescence in cancer, Nat. Rev. Cancer 14 (2014) 547–558.
 [71] R.S. Kim, A. Avivar-Valderas, Y. Estrada, P. Bragado, M.S. Sosa, J.A. Aguir-
- [71] R.S. Kim, A. Avivar-Valderas, Y. Estrada, P. Bragado, M.S. Sosa, J.A. Aguir-re-Ghiso, J.E. Segall, Dormancy signatures and metastasis in estrogen receptor positive and negative breast cancer, PLoS ONE 7 (2012) e35569.
- [72] M.S. Sosa, F. Parikh, A.G. Maia, Y. Estrada, A. Bosch, P. Bragado, E. Ekpin, A. George, Y. Zheng, H.-.M. Lam, C. Morrissey, C.-.Y. Chung, E.F. Farias, E. Bernstein, J.A. Aguirre-Ghiso, NR2F1 controls tumour cell dormancy via SOX9- and RARβ-driven quiescence programmes, Nat. Commun. 6 (2015) 6170.
- [73] M. Collado, J. Gil, A. Efeyan, C. Guerra, A.J. Schuhmacher, M. Barradas, A. Benguría, A. Zaballos, J.M. Flores, M. Barbacid, D. Beach, M. Serrano, Senescence in premalignant tumours, Nature 436 (2005) 642.
- [74] C. Neophytou, P. Boutsikos, P. Papageorgis, Molecular mechanisms and emerging therapeutic targets of triple-negative breast cancer metastasis, Front. Oncol. 8 (2018) 31.
- [75] N. Linde, G. Fluegen, J.A. Aguirre-Ghiso, The relationship between dormant cancer cells and their microenvironment, Adv. Cancer Res. 132 (2016) 45–71.
- [76] M. Spiliotaki, D. Mavroudis, K. Kapranou, H. Markomanolaki, G. Kallergi, F. Koinis, K. Kalbakis, V. Georgoulias, S. Agelaki, Evaluation of proliferation and apoptosis markers in circulating tumor cells of women with early breast cancer who are candidates for tumor dormancy, Breast Cancer Res 16 (2014) 485–485.